Computational and Structural Biotechnology Journal 21 (2023) 3315–3326

Contents lists available at ScienceDirect

Computational and Structural Biotechnology Journal

journal homepage: www.elsevier.com/locate/csbj

Current progress in artificial intelligence-assisted medical image analysis for chronic kidney disease: A literature review

Dan Zhao [a,1], Wei Wang [b,1], Tian Tang [a], Ying-Ying Zhang [a,*], Chen Yu [a,*]

[a] Department of Nephrology, Tongji Hospital, School of Medicine, Tongji University, Shanghai 200065, China
[b] Department of Radiology, Tongji Hospital, School of Medicine, Tongji University, Shanghai 200065, China

ARTICLE INFO

Article history:
Received 28 October 2022
Received in revised form 28 May 2023
Accepted 28 May 2023
Available online 30 May 2023

Keywords:
Artificial intelligence
Radiomics
Deep learning
Chronic kidney disease

ABSTRACT

Chronic kidney disease (CKD) causes irreversible damage to kidney structure and function. Arising from various etiologies, risk factors for CKD include hypertension and diabetes. With a progressively increasing global prevalence, CKD is an important public health problem worldwide. Medical imaging has become an important diagnostic tool for CKD through the non-invasive identification of macroscopic renal structural abnormalities. Artificial intelligence (AI)-assisted medical imaging techniques aid clinicians in the analysis of characteristics that cannot be easily discriminated by the naked eye, providing valuable information for the identification and management of CKD. Recent studies have demonstrated the effectiveness of AI-assisted medical image analysis as a clinical support tool using radiomics- and deep learning-based AI algorithms for improving the early detection, pathological assessment, and prognostic evaluation of various forms of CKD, including autosomal dominant polycystic kidney disease. Herein, we provide an overview of the potential roles of AI-assisted medical image analysis for the diagnosis and management of CKD.

Contents

Abbreviations: CKD, chronic kidney disease; AI, artificial intelligence; ESRD, end-stage renal disease; KDIGO, Kidney Disease Improving Global Outcomes; eGFR, estimated glomerular filtration rate; DL, deep learning; ADPKD, autosomal dominant polycystic kidney disease; QUADAS-2, Quality Assessment of Diagnostic Accuracy Studies-2; DICOM, Digital Imaging and Communications in Medicine; ROIs, regions of interest; ROC, receiver operator characteristics curve; CNN, convolution neural networks; TL, transfer learning; US, ultrasound; fMRI, functional MRI; BOLD, blood oxygen level-dependent; CT, computed tomography; TKV, total kidney volume; MRI, magnetic resonance imaging; AUC, area under the curve

* Corresponding authors.
E-mail addresses: idklaa@126.com (Y.-Y. Zhang), yuchen@tongji.edu.cn (C. Yu).

[1] These authors contributed equally to this paper

https://doi.org/10.1016/j.csbj.2023.05.029

1. Introduction

With a incidence rising faster than most other chronic diseases, chronic kidney disease (CKD) is expected to become the fifth-leading cause of death globally by 2040. Early detection and timely intervention for CKD is critical for preventing the progression to end-stage renal disease (ESRD) [1–6]. Each year worldwide, approximately 1.5 million patients with ESRD undergo dialysis while awaiting kidney transplantation, all of which contribute huge economic burdens for patients and health care systems [7].

The Kidney Disease Improving Global Outcomes (KDIGO) guidelines define CKD as abnormalities of kidney structure or function persisting for over 3 months with implications for health [8]. In clinical practice, renal dysfunction is usually marked by albuminuria or reduced estimated glomerular filtration rate (eGFR), whereas renal structural abnormalities are primarily identified by medical imaging. Early detection of CKD is often confounded by the technical challenges associated with identifying microscopic structural changes in kidney tissues, leading to the diagnosis of most CKD patients in more advanced stages of disease [9]. In recent years, studies have used artificial intelligence (AI) in the form of radiomics-based machine learning and deep learning (DL) algorithms to acquire quantitative diagnostic information from medical imaging data that cannot be easily identified by visual inspection of digitized images with the naked eye. These novel, AI-discriminated biomarkers provide an important supplement to the conventional evaluation of imaging data for improving early detection of CKD and clinical disease management.

Our review herein will describe the findings of recent studies of the application of radiomics-based machine learning and DL algorithms in AI-assisted medical image analysis for the detection, management, and prognosis of CKD, such as the diagnosis and evaluation of autosomal dominant polycystic kidney disease (ADPKD). This information was retrieved through searches of the PubMed, Embase, and Cochrane databases for relevant literature published from January 1, 2018 to January 1, 2023. The key words were targeted at different imaging modalities, as shown in Appendix 1. We also performed a manual search of the references cited in the retrieved articles to identify additional relevant research reports. We selected publications for review that met the following criteria: 1) CKD patients; 2) radiomics or DL algorithms on medical images applied for CKD assessment; 3) published in English. Studies with animals or pediatric subjects were excluded. Given the lack of quality assessment tools specifically designed for AI studies, the modified Quality Assessment of Diagnostic Accuracy Studies-2 (QUADAS-2) checklist was used to assess the quality of the enrolled articles, referring to Zheng et al. [10]. For the assessment of patients selection bias, 15 studies had a high risk of bias (56%), 1 study had a low bias (4%) and 11 studies were unclear (40%). The high risk of bias was mainly due to the lack of a randomized or consecutive sample of patients enrolled. For the domain of index, most studies (56%) were considered to have high risk of bias attributed to the lack of independent external validation. Detailed assessment results are shown in Table 1 and Fig. 1.

2. AI in medical image analysis

Applications of AI are designed to imitate human behavior and cognitive processes [11]. Given the ever-increasing breadth of data that current clinical research encompasses, including health records, diagnostic and treatment data, and extensive genomic databases, a major advantage of AI lies in its ability to efficiently analyze big data [12]. The use of AI technology has been widely accepted for diagnosis, treatment, and prognosis in a range of diseases and clinical scenarios. Studies have applied AI techniques to multiple aspects of CKD-related health care, including an alert system for identifying patients at risk for CKD onset, diagnosis based on digital imaging data, and biopsy evaluation based on DL models [11,13–15]. Among CKD-related AI applications, AI-assisted medical image analysis has been studied most extensively.

The progression of CKD is characterized by the gradual loss of renal cells with replacement by extracellular matrix proteins, resulting in fibrosis. Renal fibrosis represents a hallmark of end stage CKD that occurs independent of the etiology. The pathological features include excessive deposition of extracellular matrix proteins, peritubular capillary atrophy, and the epithelial-to-mesenchymal transition of renal tissue resulting in scarring. These pathological changes can be mapped to the heterogeneity of texture, volume, and shape of kidney tissues in digital medical images [16]. Slight differences in these image characteristics are difficult to discern visually, thereby demonstrating the utility of AI-assisted medical image analysis.

In clinical practice, various modalities are used for kidney imaging to directly observe anatomical structure or to indirectly detect pathophysiological aberrations [17–21]. Regardless of whether diagnosis is empirically based on morphological alterations or it considers traditional quantitative imaging parameters, there exists great potential for the under-utilization of valuable imaging information due simply to the limitations of human vision [22–24]. By mining imaging features and using mathematical algorithms to analyze the characteristics of training data, AI can identify and evaluate the extent of disease pathology. In medical image analysis, the use of AI is broadly divided into two categories: hand-crafted radiomics and DL.

2.1. Hand-crafted radiomics

The concept of radiomics was first proposed in 2012 by the Dutch scholar Lambin Equals. Radiomics refers to the application of mathematical methods to extract quantitative features from medical images. Learning algorithms can be designed to identify patterns in the heterogeneity and spatial distribution of pixels within predefined regions of images as selected by the user, which have been shown to reflect different disease states [25–27].

In the radiomic workflow (Fig. 2), image acquisition and preprocessing most often involve medical imaging data recorded in the Digital Imaging and Communications in Medicine (DICOM) format. Following acquisition, preprocessing removes digital noise and preserves structural information by enhancement and normalization. In image segmentation, regions of interest (ROIs) are specified for subsequent image analysis, which begins with feature extraction and selection. PyRadiomics, an open-source python package is specially designed for feature extraction applying to medical images. Several open-source software platforms can also be used to extract image features without the need for programming.

Table 1
Risk of bias assessment.

Study	Patient Selection		Index Test			Reference Standard	Flow and Timing
	Was a consecutive or random sample of patients enrolled?	Were the inclusion and exclusion criteria specified?	Were the index test results interpreted without knowledge of the results of the reference standard?	Was the validation independent?	Was the detailed imaging acquisition protocol and modeling approach?	Was the reference standard adequate?	Was there an appropriate interval between index test and reference standaed?
Bevilacqua et al.[14]	Unclear	No	Yes	Yes	Yes	Unclear	Yes
Bandara et al.[30]	Unclear	Yes	Yes	No	Yes	Yes	Yes
Ding et al.[31]	Unclear	Yes	Yes	No	Yes	Yes	Yes
Kuo et al.[40]	Unclear	Yes	Yes	Yes	Yes	Yes	Yes
Ardakani et al.[51]	Unclear	Yes	Unclear	No	Yes	Yes	Yes
Chen et al.[52]	Unclear	Yes	Unclear	No	Yes	Yes	Unclear
Iqbal et al.[53]	No	No	Unclear	No	Yes	Yes	Unclear
Hao et al.[54]	No	No	Unclear	No	Yes	Yes	Unclear
Lee et al.[55]	Unclear	Yes	Unclear	Yes	Yes	Yes	Yes
Grzywińska et al.[56]	No	No	Unclear	No	No	Yes	Yes
Kline et al.[57]	Unclear	No	Unclear	No	Yes	Yes	Yes
Li et al.[61]	Unclear	Yes	Unclear	No	Yes	Yes	Yes
Deng et al.[62]	Unclear	Yes	Unclear	No	Yes	Yes	Unclear
Rossi et al.[63]	Unclear	No	Unclear	No	Yes	Yes	Yes
Xu et al.[67]	Unclear	Yes	Yes	No	Yes	Yes	Unclear
Sabanayagam et al.[68]	Yes	No	Yes	Yes	Yes	Yes	Yes
Shi et al.[79]	Unclear	Yes	Unclear	No	Yes	Yes	Unclear
Beeman et al.[80],	No	Yes	Yes	No	Yes	Yes	Yes
Chantaduly et al.[94]	Unclear	Yes	Unclear	No	Yes	Yes	Yes
Jagtap et al.[96]	No	No	Yes	Yes	Yes	Yes	Yes
Daniel et al.[97]	No	No	Yes	Yes	Yes	Yes	Yes
Gastel et al.[98]	Yes	Yes	Yes	Yes	Yes	Yes	Yes
Sharma et al.[102]	Yes	No	Yes	Yes	Yes	Yes	Yes
Onthoni et al.[103]	Unclear	No	Yes	Yes	Yes	Unclear	Yes
Raj et al.[105]	No	No	Yes	Yes	Yes	Yes	Yes
Kline et al.[106]	Unclear	No	Yes	Yes	Yes	Yes	Yes
Sharbatdaran et al.[107]	No	No	Yes	Yes	Yes	Yes	Yes

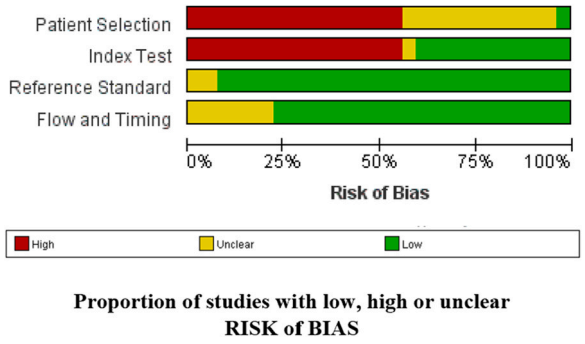

Fig. 1. Risk of bias assessments of selected publications through the modified QUADAS-2. QUADAS-2: Quality Assessment of Diagnostic Accuracy Studies-2.

Radiomics features are typically categorized as statistical (including texture-based and histogram-based), transform-based, model-based, or shape-based features, which represent different types of information that are extracted directly or statistically calculated from the imaging data (Table 2) [28,29].

Much of the information contained within the acquired features might not be associated with target variables [30]. Feature reduction, which most often uses linear discriminant or principal component analysis, removes irrelevant or redundant information in features, and combines multiple relevant features into new, individual features. Multiple characteristics of the resulting features serve as designated imaging biomarkers, which are often then analyzed to build prediction models using machine learning algorithms, known as a branch of AI. The algorithm is chosen based on the type of target variable (categorical or continuous) and certain data characteristics, such as sample size, dimensions, and so on, as well as the experience and preferences of the clinician.

Model validation is also an integral part of a comprehensive radiomics analysis, especially external validation in large, independent, prospective datasets. The receiver operator characteristics curve (ROC), sensitivity, and specificity can also be used to evaluate model performance. Radiomics analyses based on different medical imaging modalities have been used for the diagnosis of a wide range of diseases, thereby demonstrating the power of computer-aided diagnostic tools [31–34]. However, potential limitations lie in the predefined nature of radiomic features and their dependency on the current domain of knowledge. Therefore, the full advantages of AI for developing diagnostic tools through the analysis of big data might not be perfectly represented due to the handcrafting of features.

2.2. DL

The branch of AI known as DL uses multiple layers of artificial neural networks with interconnecting nodes that simulate learning and cognition in the human brain. Convolution neural networks (CNN) are DL neural networks with a convolution structure that simulates information processing in the human visual cortex [35–37].

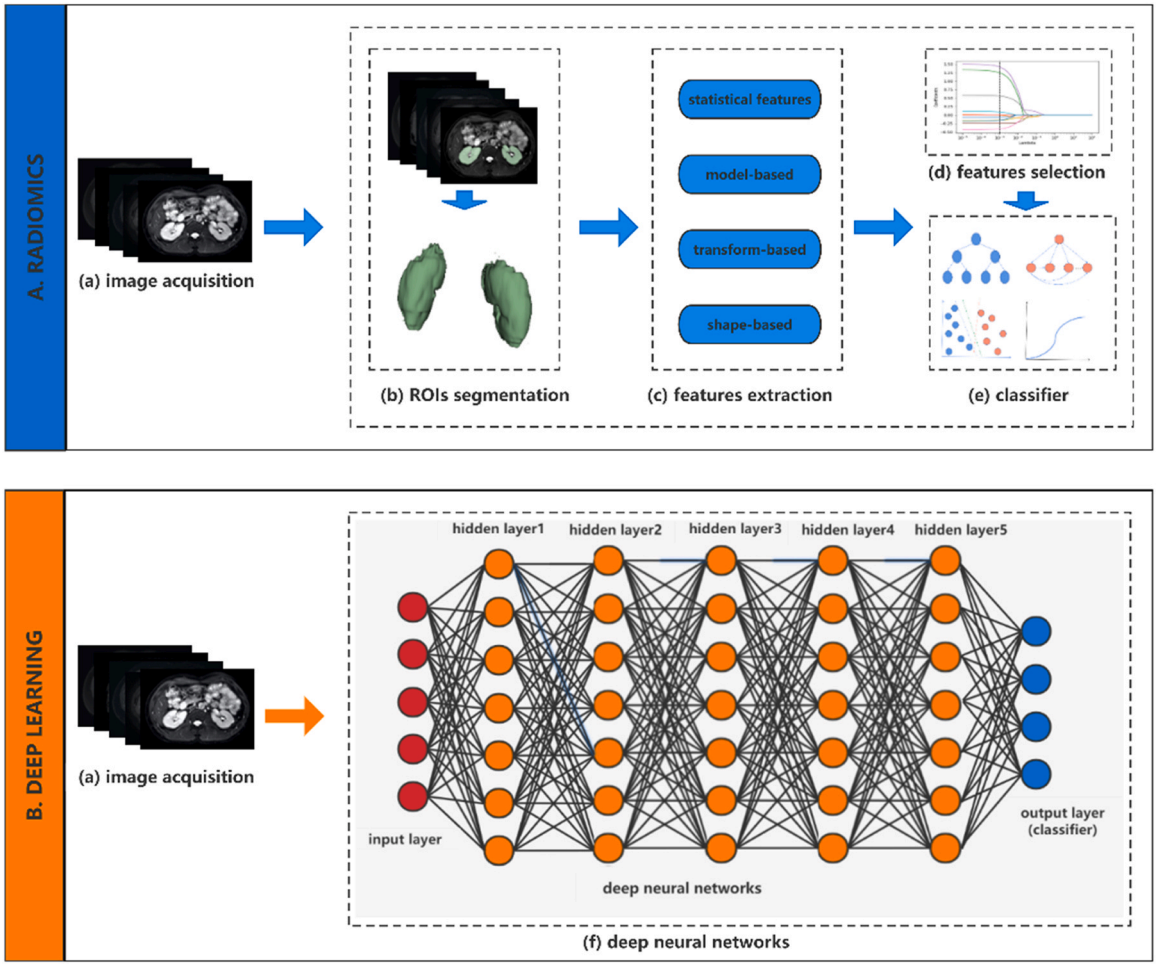

Fig. 2. Flowchart of radiomics and deep learning. (A). Basic steps in radiomics, including medical images acquisition, regions of interest (ROIs), features extraction, features selection and classifier construction. (B) Deep learning directly generates deep neural networks (f) after medical image acquisition, replacing steps b-e in radiomics in Figure A, thus enabling end-to-end learning.

Table 2
Classification and description of radiomic features.

Classification	Description
first-order	describing the distribution of pixels or voxels in an image, including minimum, maximum, mean, median, range, etc.
Texture-based	describing the relationship of pixels or voxels in an image, including GLCM, GLRLM, GLSZM, NGTDM, GLDM and Absolute Gradient.
Model-based	A parameterized model of texture generation is calculated and fitted to the ROIs, and the estimated parameters are used as radiomic features.
Transform-based	extracting features from the transformed images, including fourier transform, Gabor transform, wavelet transform, laplace transform, etc.
Shape-based	describing the geometric properties of ROIs, including diameter, shaft, volume, area, ratio, etc.

Abbreviation: GLCM, Gray-level Co-occurrence Matrix; GLRLM, Gray-level Run-length Matrix; GLSZM, Gray-level Size Zone Matrix; NGTDM, Gray-level Size Zone Matrix; GLDM, Gray level dependence matrix; ROIs: regions of interest;

Using the whole image as a direct input to the network, the CNN automatically extracts features using the deep convolution and pooled sampling layers, avoiding the manual feature extraction and data reconstruction of traditional radiomics analysis (Fig. 2). With the deepening of network layers, higher-level abstract features can be learned that improve the sensitivity of identification. Compared with traditional radiomics, CNNs are more automated due to the implementation of end-to-end learning patterns throughout the training process, from image input to recognition output, without the need for human intervention [38]. A comparison of radiomics and DL is summarized in Table 3.

Transfer learning (TL) is a new framework based on DL that aims to solve the fundamental problem of insufficient training data. Based on the similarity between the source task and target task, model parameters can be obtained by pretraining on a source task comprising a larger data set, and these parameters are then migrated to the target task with a smaller sample size to construct a robust CNN model [39]. Various factors contribute to the difficulty associated with acquiring a large sample of renal images, such as the comparatively low prevalence of CKD, the skewed distribution of patients toward advanced disease, and the lack of a universal kidney image-sharing platform. Hence, TL can enhance the potential benefit of AI-based image analysis for CKD patients [40].

The rapid development of DL has brought innovation to traditional radiomics. The segmentation of ROIs using DL algorithms increases the automation of radiomics [41–44]. A recently described radiomics method uses a deep transfer network in the feature extraction algorithm, thereby replacing or integrating handcrafted features, which not only reduces the amount of data required, but also provides the advantages of DL [45–47]. Zheng et al. [48] demonstrated that classification of kidney ultrasound (US) images based on a combination of TL and handcrafted features was more effective than that based on TL or handcrafted features alone. In the future, AI will bring more innovations and breakthroughs in this type of medical image analysis.

3. AI-assisted medical image analysis in CKD

3.1. Evaluation of renal function

As CKD is usually occult at onset, regular screening of renal function is highly recommended by the American Society of Nephrology [49,50]. At present, serum creatinine and albuminuria are the most commonly accepted biomarkers for CKD screening, but neither provides accurate assessment of glomerular structural integrity. AI-based medical image analysis can use eGFR or serum creatinine as ground truth references for the development of models for noninvasive renal function assessment.

3.1.1. US-based evaluation of renal function

The availability, cost-effectiveness, and convenience of medical US make it a first-line diagnostic tool in nephrology. Moreover, compared to some techniques, it does not expose patients to ionizing radiation. Ardakani et al. [51] were the first researchers to apply radiomics to the analysis of renal US images in the diagnosis of renal failure after transplantation. For each ROI, they extracted up to 270 texture features, 14 of which were closely associated with the level of serum creatinine. Chen et al. [52] built support vector machine models based on the grey level co-occurrence matrix (GLCM) of renal US images that demonstrated an accuracy of 75.95% in discriminating CKD stages 1–5. Studies have also used transformed-based features extracted from US images. Bandara et al. [30] extracted second-order features from wavelet-transformed images to identify CKD. They found that the 10 most significant features were sensitive to the directionality of US speckle patterns. Iqbal et al. [53] demonstrated that Fourier transform-based features reflecting spatial frequencies could successfully identify patients with CKD, whereas the GLCM-based features could not.

To date, all DL models for evaluating renal dysfunction have been based on US images. A US-based CNN model developed by Kuo et al. [40] demonstrated a high proficiency for identifying CKD (eGFR < 60 ml/min/1.73 m^2; AUC = 0.904, specificity = 92.1%, and accuracy = 85.6%), surpassing that of experienced nephrologists and traditional machine learning models. A novel CNN framework was also proposed by Hao et al. [54] in which texture branching was introduced into the CNN network, simultaneously extracting texture features and new deep features from input images, which demonstrated an accuracy of 96.01% and a sensitivity of 99.44%. Lee et al. [55] introduced measurable features and clinical variables into a CNN network which also improved the accuracy of identifying CKD.

3.1.2. Magnetic resonance imaging (MRI)-based evaluation of renal function

MRI has become the most common second-line imaging option for evaluating CKD, due in large part to its high resolution of soft tissues, the lack of ionizing radiation, and multiple sequence choices.

Table 3
Comparison of radiomics and deep learning.

	Radiomics	Deep learning
sample size	less label data relatively	demanding large label data, usually through transfer learning, data augmentation, etc.
features extraction	predefined or hand-crafted quantitative features	massive layered features derived from autonomous learning of neural networks
classifier	conventional statistical or machine learning models	deep neural networks
Image segmentation	drawing regions of interest manually	The whole images can be used as direct input
interpretability	results can be attributed to single predictor included in machine learning models	"black box" models mostly, which can be explained by shaply-value, etc.

Grzywińska et al. [56] explored the relationship between renal function and radiomics features from T2WI images. They found that features from the renal cortex were more significantly associated with serum creatinine level and eGFR, compared with that of the whole kidney, which could be attributed to the abundance of functional glomeruli in the cortex. Building upon such findings, Kline et al. [57] combined radiomic features extracted from T2WI images with age, baseline eGFR, and total kidney volume to construct a multivariable linear regression model that successfully predicted the risk of CKD progression to stage 3 in ADPKD patients after 8 years of follow-up.

Compared with traditional MRI technology, emerging functional MRI (fMRI) can better reflect micropathophysiological changes, and has greater potential to evaluate renal dysfunction. Numerous studies [58–60] have confirmed that conventional quantitative fMRI parameters are significantly correlated with indicators of renal function, such as serum creatinine, albuminuria, and eGFR. However, these parameters reflect only the average signal strength within the selected ROIs, and do not mine abundant hidden information in fMRI images. Studies have investigated whether AI-based fMRI analysis can provide a better assessment of renal dysfunction. Li et al. [61] performed a diffusion-weighted imaging-based radiomics analysis of fMRI. They constructed a logistic regression model to distinguish patients with CKD from healthy individuals that demonstrated a sensitivity of 93% and specificity of 70%.

Ding et al. [31] compared the use of radiomic features from susceptibility-weighted imaging, blood oxygen level-dependent (BOLD) imaging, and diffusion-weighted imaging data to discriminate between different stages of CKD. Their results showed that the use of features extracted from BOLD and susceptibility-weighted imaging data demonstrated similar discriminating abilities, and were more suitable for early recognition of renal dysfunction, compared with that of diffusion-weighted imaging. Deng et al. [62] and Rossi et al. [63] explored the use of feature extractions from diffusion tensor imaging and arterial spin-labelling MRI, respectively, and both demonstrated proficiency for the early detection of CKD. However, considering the limited sample sizes of these studies, the ability of AI-based fMRI analyses to evaluate renal dysfunction requires further validation in large-scale clinical studies Tables 4–6.

3.1.3. Computed tomography (CT)-based evaluation of renal function

To date, relatively few studies have reported the use of AI-assisted CT image analysis for renal function assessment. One study explored the effectiveness of AI-assisted CT image analysis for predicting radiation-induced CKD in patients undergoing radiation therapy for abdominal tumors [33]. Due to the exposure of patients to ionizing radiation, the use AI-assisted CT assessment might be limited to specific types of patients, rather than for continuous monitoring of renal function status in all types of CKD patients.

3.1.4. Retinal imaging-based evaluation of renal function

Some recent studies of the evaluation of renal function have shifted focus to AI-assisted retinal imaging analysis due to the similarity of pathophysiological changes that occur in both the retinal and renal microcirculations during the early stages of diabetes. Patients with microvascular retinal signs are also more likely to develop CKD in clinical practice, suggesting that retinal imaging might provide supplementary information for CKD screening [64–66]. Xu et al. [67] analyzed retinal images from 1925 patients with type 2 diabetes, and found that texture features reflecting enhanced homogeneity and contrast were strongly associated with renal dysfunction. Sabanayagam et al. [68] built a CNN model based on retinal images to detect CKD, resulting in an AUC of 0.911. This model was also validated in two independent cohorts with AUCs of 0.835 and 0.733. These studies provide a new direction for the identification of renal dysfunction. The integration of CKD screening into the retinal imaging-based screening of diabetes patients not only improves the efficiency and cost-effectiveness of the process, it also improves early detection of renal disease in high-risk populations [3].

3.2. Pathological diagnosis of CKD

Renal tissue pathology provides an objective basis for etiological determination, prognosis, and personalization of treatment [69,70]. With advancements in digital pathology, whole-slide image technology allows high-resolution scans of complete tissue biopsy slides that can also be subjected to AI-based images analysis. Examples of applications of AI in digital pathology include the detection and segmentation of kidney structures, the auxiliary diagnosis of renal pathological changes, and CKD prognosis [71–74]. The application of AI to whole-slide image analysis increases the power of detecting subtle changes, compared with visual assessment by clinicians, and overcomes the subjectivity of manual classification induced by differences in visual perceptions and preference. However, methods requiring biopsy are not ideal for evaluating CKD due to the invasiveness and risks of hemorrhage, arteriovenous fistula, and infection [75–78]. Needle biopsy acquires less than 1% of the kidney tissue volume, providing limited evidence of the overall pathological changes that may be present in the entire kidney. Therefore, AI technology has been primarily used for noninvasive pathological diagnosis based on medical imaging results.

3.2.1. Identification of micropathological changes

The examination of renal tissue biopsy can provide important information regarding glomerular number, micromorphology, microvascular pathology, and cell proliferation to guide etiological determination, treatment choices, and prognosis of CKD. Shi et al. [79] constructed a Fisher linear discriminant formula based on GLCM features extracted from BOLD MRI images of patients with lupus nephritis. Their model correctly identified the pathologic types of 77.8% of the biopsy samples from lupus nephritis patients, providing guidance for therapeutic decisions and prognosis. Beeman et al. [80] used non-toxic cationic ferritin as an MRI contrast agent to evaluate the number and volume of glomeruli in the kidneys of patients based on texture analysis, and demonstrated the ability to identify glomerular pathology in patients with CKD. AI-based medical image analysis for the pathological diagnosis of CKD is presently in the early stages of development. The existing studies have, however, already shown broad prospects for clinical translation of these techniques.

3.2.2. Diagnosis of renal fibrosis

Arising from various etiologies, tissue fibrosis is a fundamental pathological change contributing to CKD onset and a major risk factor for CKD progression to ESRD [81–84]. In recent years, AI-based medical image analysis has been explored primarily for the detection of tissue fibrosis of the liver [85–87]. Radiomics and DL features derived from MRI and CT images have been shown to be strongly associated with the extent of fibrosis in liver disease, and have demonstrated diagnostic proficiencies superior to the evaluation of traditional imaging biomarkers by clinicians [88–93]. Chantaduly et al. [94] were the first to use DL-based analysis for the noninvasive detection of renal fibrosis. They developed two different CNN models for kidney CT images that distinguished mild fibrosis from severe fibrosis (< 50% fibrosis versus ≥ 50% fibrosis) with greater than 85% accuracies for both classifications. This provides a promising starting point for future advancements in AI-assisted imaging analysis for the noninvasive diagnosis of renal fibrosis.

Table 4
Radiomics and deep learning in renal function evaluation.

Study	Purpose	Sample Size	Imaging Modality	Classifier	Results	Repositories
Rossi et al.[63], 2012	Discrimining patient with mild renal dysfunction staging from CKD-I to CKD-III and healthy volunteers	CKD I -III (n = 9), healthy control group (n = 8)	ASL	absent	Significant correlations between histogram-based radiomic features of the cortex and renal dysfunction.	not publicly available
Iqbal et al.[53], 2017	Discriminating CKD patients form healthy volunteers	Patients with CKD (n = 8), and healthy control group (n = 24)	US	absent	Fourier-based radiomic features could distinguish healthy and CKD kidneys successfully.	not publicly available
Ardakani et al. [51], 2017	Identifing renal dysfunction after allograft transplantation.	Renal allograft rejected (n = 39), non-rejected (n = 55)	US	First nearest neighbor	Fourteen texture features were showed as significant correlation with eGFR and 16 were significantly different between the rejected and non-rejected allografts.	not publicly available
Kline et al.[57], 2017	Prediction of the progression to CKD stage 3 A, 3B and 30% reduction of eGFR for patient with ADPKD	CKD stage 3 A (n = 44), 3B (n = 22), and 30% reduction of eGFR (n = 47)	T2WI	Multiple linear regression	Textural parameters improved the prediction power of progression to CKD 3 A, 3B and were well correlated to eGFR changes.	not publicly available
Ding et al.[31], 2019	Exploring the value of texture analysis based on DWI, BOLD, and SWI in evaluating renal dysfunction	eGFR < 30(n = 31), eGFR 30–80(n = 24), and eGFR≥ 80(n = 17)	DWI, BOLD and SWI	absent	Compared with DWI, texture features derived from BOLD and SWI may be more suitable for assessing renal dysfunction during early stages, and have similar discriminating abilities.	not publicly available
Hao et al.[54], 2019	Discriminating CKD patients from healthy individuals	CKD (n = 180), healthy (n = 46)	US	texture branch network	The accuracy and sensitivity of texture branch network was 96.01%, 99.44% respectively.	not publicly available
Kuo et al.[40], 2019	Developing a deep learning approach for automatically determining the eGFR and CKD status	4.505 us images of 1297 patients (training set : n = 4010 ; testing set : n = 495)	US	ResNet101 ; Xgboost	The developed deep learning model was able to identify the CKD status defined by an eGFR of < 60, with AUC of 0.904, specificity of 92.1%, and accuracy of 85.6% higher than that of experienced nephrologists.	not publicly available
Chen et al.[52], 2020	Predicting of CKD stage (I to V) for CKD patients	CKD stage 1–5 (n = 205)	US	SVM	Compared with bilateral and left kidneys, radiomic features of right kidneys achieved the best prediction accuracy	not publicly available
Deng et al.[62], 2020	Using radiomic features based on DTI to detect early kidney damage in diabetic patients	Type 2 diabetic patients (n = 30), and healthy (n = 28)	DTI	LASSO regression model	Texture features derived from DTI MRI could detect early renal dysfunction in diabetic patients, with an AUC of 0.882.	not publicly available
Sabanayagam et al. [68], 2020	Developing an artificial intelligence deep learning algorithm to detect CKD from retinal images	Controls (eGFR≥60, n = 5267), patients with CKD (eGFR < 60, n = 1218)	Digital retinal images	cCondenseNet	The retinal images-based CNN model had good identification ability, with AUC of 0.911, 0.733 and 0.835 in three validation cohorts. Risk factors could provide additional information for the model and further improve its effectiveness.	not publicly available
Grzywińska et al. [56], 2020	Applying texture analysis to assess renal function after kidney transplantation	Renal transplant recipients (n = 9)	T2WI	absent	Significant correlations between the texture parameters and eGFR	not publicly available
Xu et al.[67], 2021	Exploring the ability of the retinal vasculature as potential biomarker for the early identification of those at high risk of CKD in diabetes.	CKD (n = 249), non-CKD (n = 1676)	Digital retinal images	absent	Texture analysis of retinal imaging revealed that renal dysfunction in type 2 diabetes was associated with various retinal image measurements, such as increased homogeneity and contrast.	not publicly available
Bandara et al. [30], 2021	Discriminating CKD patients form healthy volunteers	Patients with CKD (n = 75), and healthy (n = 27)	US	SVM	All top 10 radiomics features identified in this study were based on the wavelet transformation, and WT (LH) GRLN appeared to be robust in capturing speckle features that are faithful to the kidney anatomy.	not publicly available
Li et al.[61], 2022	Discrimination between healthy individuals and CKD patients (eGFR < 60)	CKD (eGFR < 60, n = 30) , and healthy (n = 10)	DWI	hierarchical clustering, LR	Five radiomic features could identify CKD patients, with a sensitivity of 93%, specificity of 70%, and an AUC of 0.95. Similarly, four radiomic features were able to classify participants as rapid vs. non-rapid CKD progressors with a sensitivity of 71%, specificity of 43%, and an AUC of 0.75.	not publicly available

(*continued on next page*)

Table 4 (*continued*)

Study	Purpose	Sample Size	Imaging Modality	Classifier	Results	Repositories
Lee et al.[55], 2022	Discriminating CKD patients from non-CKD by integrating computer-extracted measurable features with the CNN based on ultrasound images	CKD (n = 350), and non-CKD (n = 489)	US	ResNet18	The average AUC of CNN model based on US images achieved a level of 0.81. Image training with the integration of automatically extracted measured features revealed an improved average AUC of 0.88.	not publicly available

Abbreviation: CKD: chronic kidney disease; ASL: arterial spin labeling; US: ultrasound; eGFR: estimated glomerular filtration rate; ADPKD: Autosomal dominant polycystic kidney disease; DWI: diffusion-weighted imaging; BOLD: blood oxygen level-dependent magnetic resonance imaging; Xgboost: eXtreme gradient boosting; SVM: Support Vector Machine; CNN: convolutional neural network; AUC: Area Under the Curve; CT: Computed tomography; WT(LH) GRLN: wavelet transformed (LH) Gray Level Dependence Matrix; LR: logistic regression; DT: Decision Tree; GBDT: Gradient Boosting Decision Tree; k-NN: k-Nearest Neighbor;

Table 5
Medical image AI analysis in renal pathology.

Study	Purpose	Sample Size	Imaging Modality	Classifier	Results	Repositories
Beeman et al. [80], 2014	Utilizing cationized ferritin (CF) as a MRI contrast agent to measure nephron number and size in viable human kidneys	n = 3	MRI	absent	The distribution of CF-labeled glomeruli may be predictive of glomerular and vascular disease.	not publicly available
Shi et al.[79], 2018	Determining whether BOLD MRI can contribute to the diagnosis of renal pathological patterns	healthy (n = 11), LN patients (n = 12), divided into four subgroups of pathology (classIII,classIII+V,classIV,classIV+V)	BOLD MRI	Fisher linear discrimination	GLCM analysis could detect the differences in the texture characteristics of BOLD MRI in different pathotypes of LN patients, with an accuracy of 77.8%.	not publicly available
Chantaduly et al. [94], 2022	Distinguishing between severe and mild / moderate renal fibrosis	Mild fibrosis (< 25%, n = 55), moderate (25%–50%, n = 14), and severe (> 50%, n = 23)	CT	slicer-level CNN; Voxel-level CNN	The two CNN models demonstrated similar positive predictive value (0.886 versus 0.935) and accuracy (0.831 versus 0.879).	not publicly available

Abbreviation: AI: artificial intelligence; MRI: magnetic resonance imaging; BOLD: blood oxygen level-dependent; GLCM: Gray-level Co-occurrence Matrix; LN: lupus nephritis; CT: Computed tomography; CNN: convolutional neural network;

Table 6
Deep learning in Autosomal dominant polycystic kidney disease.

Study	Sample Size	Imaging Modality	Classifier	Results	Repositories
Sharma et al.[102], 2017	Training: n = 165 Testing: n = 79	CT	CNN	The CNN model facilitated fast and reproducible measurements of kidney volumes in agreement with manual segmentations from clinical experts.	not publicly available
Gastel et al.[98], 2019	Training: n = 440 Testing: n = 100	T2WI	DL	The fully automated segmentation method that measured TKV, TLV, and changes in these parameters as accurately as manual tracing.	not publicly available
Bevilacqua et al.[14], 2019	Training: n = 165 Testing: n = 79	T1WI	R-CNN	Both CNN models were reliable for the semantic segmentation of polycystic kidneys with an accuracy higher than 85%.	not publicly available
Onthoni et al.[103], 2020	Training: n = 88 Testing: n = 22	Contrast enhanced CT	CNN	The contstructed model outperformed other DL detectors in terms of AP and mAP.	not publicly available
Daniel et al.[97], 2021	Training: n = 50 Testing: n = 50	T2WI	U-Net	The 2D CNN method provides fully automated segmentation of the left and right kidney and calculation of TKV in < 10 s	not publicly available
Kim et al.[104], 2022	Training: n = 157 Testing: n = 53	T2WI	3D U-Net	The model was able to measure TKV that excluded exophytic cysts and had an accuracy similar to that of a human expert.	not publicly available
Raj et al.[105], 2022	CKD stage 1–3 (n = 100)	T1WI	U-Net	Combining loss and SAM could achieve better accuracy in small datasets	https://repository.niddk.nih.gov/studies/crisp1/
Kline et al.[106], 2022	Training: n = 40 Testing: n = 20	T2WI	CNN	The accuracy of kidney segmentation and volume calculation in the CNN model was similar to that of 2 readers	not publicly available
Jagtap et al.[96] , 2022	N = 22	3D US	CNN	Using 3D US to measure TKV for auto-segmentation of kidneys showed promising performance, close to human tracing and MRI measurement.	not publicly available
Sharbatdaran et al.[107] , 2022	Training: n = 151 Testing: n = 64 Validating: n = 60	T2WI	2D U-Net	The method reduced the time required to perform multiorgan segmentations in ADPKD and reduced measurement variability	not publicly available

Abbreviation: CT: Computed tomography; CNN: convolutional neural network; DL: deep learning; TKV: total kidney volume; AP: average precision; mAP: mean average precision; SAM: sharpness aware minimization; US: ultrasound; ADPKD: Autosomal dominant polycystic kidney disease.

3.3. Evaluation of ADPKD

Total kidney volume (TKV) is an important imaging biomarker for assessing the severity and progression of ADPKD[57,95]. However, computing TKV is challenging due to the high degree of variability caused by the abnormal growth of polycystic kidneys. Despite a high level of accuracy, traditional TKV calculation relies on manually tracking the kidney boundaries, which is time-consuming and susceptible to inter- and intraoperator variability. By learning from input images, DL networks can accurately discriminate between renal parenchyma and pathological cysts, without the need for manual tracking, producing estimates comparable to that of automated kidney segmentation for TKV computation. Recent studies have applied DL algorithms to US, CT, and MRI imaging modalities to calculate TKV in ADPKD patients, achieving high levels of accuracy that were similar those of manual methods. Japtop et al. [96] developed a CNN model based on three-dimensional US images for the segmentation of polycystic kidney regions for TKV computation that achieved a Dice score of 0.80 in the test set. Daniel et al. [97], Gastel et al. [98] and Kim et al. [99] constructed different deep learning (DL) network models based on T2-weighted (T2WI) magnetic resonance imaging (MRI) imaging respectively, and all of their Dice coefficients could reach more than 0.90. Among them, Gastel et al. [98] extended their techniques to segment the liver and hepatic cysts in autosomal dominant polycystic kidney disease (ADPKD) patients and constructed an efficient and accurate model that could simultaneously calculate the liver and kidney volume. On the basis of accurate segmentation of renal parenchyma and cysts, further signal intensity or texture analysis of cysts can be performed for identifying complex structures of cysts, which assists in disease classification.

4. Future prospects

To date, the application of novel quantitative imaging biomarkers obtained by AI methods for CKD assessment has been studied in a preliminarily fashion. And it is fair to say that the predictive accuracy of existing models has not met the clinical needs. In order to construct more robust models and transform them into efficient and accurate computer-aided diagnosis and treatment tools, future research will focus on the following directions.

First, standardization of image acquisition: Since image quality is a key factor in AI-based medical image analysis, the image acquisition process should be normalized through standardized protocols that reduce noise interference caused by image heterogeneity, which will be particularly important in future multicenter clinical studies.

Second, data sharing: It has been shown that sample size for machine training is positively correlated with the robustness of the constructed models, but most of them are built on retrospective studies involving single center small samples, so even if the models perform well in the original training set, the generalization of performance with other sample sets remains limited. The future aim is to unlock data silos by developing a multicenter image-sharing platform or the Grand Challenges (such as KiTS21, KiTS19 for segmentation of kidney tumor) for renal imaging in CKD patients, which will facilitate the emergence of more models with high accurate and robust.

Third, pattern diversification: Novel imaging biomarkers extracted from single modality renal images alone are far from sufficient to assess CKD, so it will be necessary to continue to explore whether the combination of features obtained from multiple modalities, including the combination of features based on multimodality-based renal images extraction, the combination of radiomics and depth features, and the combination of imaging biomarkers and clinical information, can further improve the model power.

Fourth, process automation: A small number of studies [100–102] have applied the kidney autonomous segmentation algorithm to preliminarily realize the "end-to-end" automatic evaluation process, which may help to apply these AI models in areas with limited health care resources in the future and realize remote diagnosis and treatment, to meaningfully advance the noninvasive evaluation of CKD nationwide.

Fifth, Refinement of research: The research of AI-based medical image analysis in the field of CKD has mainly contributed to the assessment of renal function status and shown great potential for this application, thus future studies should focus on the molecular level to map out the association between novel imaging biomarkers and microscopic pathological changes to provide a basis for the personalized diagnosis and treatment of CKD.

5. Conclusions

The early detection and evaluation of CKD has long been problematic due to the limitations of traditional imaging and biopsy methods. With the arrival of the big data era, the application of AI technology to existing imaging modalities can improve the diagnostic value of imaging procedures. AI-based analysis of kidney US data is the most common AI-assisted imaging technique used in the field of CKD due to its cost-effectiveness and wide availability. These qualities make AI-assisted US a prime candidate for use in mobile telecare and telemedicine, and promote its introduction in settings with limited health care resources, thus improving the efficiency and sustainability of health care systems. In clinical scenarios in which the need for high resolution imaging justifies greater health care expenditures, such as the pathological classification of CKD and the investigation of pathophysiological mechanisms, AI-assisted MRI can provide optimal improvement in diagnostic imaging results. Though AI-based medical image analysis holds great promise for CKD diagnosis and management, the development of algorithms suitable for routine clinical application will require nephrologists to work together for the standardization of image acquisition specifications, improvement of image-sharing platform accessibility, and validation of these techniques in multicenter prospective studies.

CRediT authorship contribution statement

Dan Zhao, Wei Wang and Tian Tang wrote the manuscript; Ying-Ying Zhang revised the manuscript; Chen Yu guided and designed the work.

Declaration of Competing Interest

The authors declared no potential conflicts of interest with respect to the research, author- ship, and/or publication of this article.

Acknowledgements

This work was supported by the National Natural Science Foundation of China (No. 82170696, 81900622 and 82270777) and the Shanghai ShenKang Hospital develop center Project (No. SHDC12022104). This work was also supported by the Kidney Blood Purification Innovation Alliance (CKD-MBD) Youth Research Project (No. NBPIA20QC0101) and Project of Tongji Hospital of Tongji University (No. ITJ(QN)2104 and GJPY2127).

Appendix A. Supporting information

Supplementary data associated with this article can be found in the online version at doi:10.1016/j.csbj.2023.05.029.

References

[1] Zhang L, Wang F, Wang L, et al. Prevalence of chronic kidney disease in China: a cross-sectional survey. Lancet 2012;379(9818):815–22.
[2] Hoerger TJ, Simpson SA, Yarnoff BO, et al. The future burden of CKD in the United States: a simulation model for the CDC CKD Initiative. Am J Kidney Dis: J Natl Kidney Found 2015;65(3):403–11.
[3] Komenda P, Ferguson TW, Macdonald K, et al. Cost-effectiveness of primary screening for CKD: a systematic review. Am J Kidney Dis: J Natl Kidney Found 2014;63(5):789–97.
[4] Hallan SI, Dahl K, Oien CM, et al. Screening strategies for chronic kidney disease in the general population: follow-up of cross sectional health survey. BMJ (Clin Res Ed) 2006;333(7577):1047.
[5] Kalantar-Zadeh K, Jafar TH, Nitsch D, et al. Chronic kidney disease. Lancet 2021;398(10302):786–802.
[6] Thomas B, Matsushita K, Abate KH, et al. Global cardiovascular and renal outcomes of reduced GFR. J Am Soc Nephrol: JASN 2017;28(7):2167–79.
[7] Reiss AB, Miyawaki N, Moon J, et al. CKD, arterial calcification, atherosclerosis and bone health: inter-relationships and controversies. Atherosclerosis 2018;278:49–59.
[8] Eknoyan G, Lameire N, Eckardt K, et al. KDIGO 2012 clinical practice guideline for the evaluation and management of chronic kidney disease. Kidney Int 2013;3(1):5–14.
[9] Caroli A, Remuzzi A, Lerman LO. Basic principles and new advances in kidney imaging. Kidney Int 2021;100(5):1001–11.
[10] Zheng X, He B, Hu Y, et al. Diagnostic Accuracy of Deep Learning and Radiomics in Lung Cancer Staging: A Systematic Review and Meta-Analysis. Front Public Health 2022;10:938113.
[11] Yuan Q, Zhang H, Deng T, et al. Role of artificial intelligence in kidney disease. Int J Med Sci 2020;17(7):970–84.
[12] Fleming N. How artificial intelligence is changing drug discovery. Nature 2018;557(7707):S55–7.
[13] Tomašev N, Glorot X, Rae JW, et al. A clinically applicable approach to continuous prediction of future acute kidney injury. Nature 2019;572(7767):116–9.
[14] Bevilacqua V, Brunetti A, Cascarano GD, et al. A comparison between two semantic deep learning frameworks for the autosomal dominant polycystic kidney disease segmentation based on magnetic resonance images. BMC Med Inf Decis Mak 2019;19(Suppl 9):244.
[15] Tey WK, Kuang YC, Ooi MP, et al. Automated quantification of renal interstitial fibrosis for computer-aided diagnosis: a comprehensive tissue structure segmentation method. Comput Methods Prog Biomed 2018;155:109–20.
[16] Zhang J, Zhang LJ. Functional MRI as a tool for evaluating interstitial fibrosis and prognosis in kidney disease. Kidney Dis 2020;6(1):7–12. https://doi.org/10.1159/000504708
[17] Yuan Q, Zhang H, Deng T, et al. Role of artificial intelligence in kidney disease. Int J Med Sci 2020;17(7):970–84.
[18] Fleming N. How artificial intelligence is changing drug discovery. Nature 2018;557(7707):S55–7.
[19] Tomašev N, Glorot X, Rae JW, et al. A clinically applicable approach to continuous prediction of future acute kidney injury. Nature 2019;572(7767):116–9.
[20] Roussel E, Capitanio U, Kutikov A, et al. Novel imaging methods for renal mass characterization: a collaborative review. Eur Urol 2022;81(5):476–88.
[21] Tey WK, Kuang YC, Ooi MP, et al. Automated quantification of renal interstitial fibrosis for computer-aided diagnosis: a comprehensive tissue structure segmentation method. Comput Methods Prog Biomed 2018;155:109–20.
[22] Lucisano G, Comi N, Pelagi E, et al. Can renal sonography be a reliable diagnostic tool in the assessment of chronic kidney disease? J Ultrasound Med: J Am Inst Ultrasound Med 2015;34(2):299–306.
[23] Yaprak M, Çakır Ö, Turan MN, et al. Role of ultrasonographic chronic kidney disease score in the assessment of chronic kidney disease. Int Urol Nephrol 2017;49(1):123–31.
[24] Wieczorek AP, Woźniak MM, Tyloch JF. Errors in the ultrasound diagnosis of the kidneys, ureters and urinary bladder. J Ultrason 2013;13(54):308–18.
[25] Alnazer I, Bourdon P, Urruty T, et al. Recent advances in medical image processing for the evaluation of chronic kidney disease. Med Image Anal 2021;69:101960.
[26] Castellano G, Bonilha L, Li LM, et al. Texture analysis of medical images. Clin Radiol 2004;59(12):1061–9.
[27] Ortiz-Ramón R, Larroza A, Ruiz-España S, et al. Classifying brain metastases by their primary site of origin using a radiomics approach based on texture analysis: a feasibility study. Eur Radiol 2018;28(11):4514–23.
[28] Lambin P, Leijenaar RTH, Deist TM, et al. Radiomics: the bridge between medical imaging and personalized medicine. Nat Rev Clin Oncol 2017;14(12):749–62.
[29] Mayerhoefer ME, Materka A, Langs G, et al. Introduction to radiomics. J Nucl Med: Publ, Soc Nucl Med 2020;61(4):488–95.
[30] Bandara MS, Gurunayaka B, Lakraj G, et al. Ultrasound based radiomics features of chronic kidney disease. Acad Radio 2022;29(2):229–35.
[31] Ding J, Xing Z, Jiang Z, et al. Evaluation of renal dysfunction using texture analysis based on DWI, BOLD, and susceptibility-weighted imaging. Eur Radio 2019;29(5):2293–301.
[32] Chen X, Huang X, Yin M. Implementation of hospital-to-home model for nutritional nursing management of patients with chronic kidney disease using artificial intelligence algorithm combined with CT internet. Contrast Media Mol Imaging 2022;2022:1183988.

[33] Amiri S, Akbarabadi M, Abdolali F, et al. Radiomics analysis on CT images for prediction of radiation-induced kidney damage by machine learning models. Comput Biol Med 2021;133:104409.
[34] Ardakani AA, Hekmat S, Abolghasemi J, et al. Scintigraphic texture analysis for assessment of renal allograft function. Pol J Radiol 2018;83:e1–10.
[35] Chartrand G, Cheng PM, Vorontsov E, et al. Deep learning: a primer for radiologists. Radio: a Rev Publ Radiol Soc North Am, Inc 2017;37(7):2113–31.
[36] LeCun Y, Bengio Y, Hinton G. Deep learning. Nature 2015;521(7553):436–44.
[37] Lemley KV. Kidney fibrosis assessment by CT using. Mach Learn Kidney360 2022;3(1):1–2.
[38] Dana J, Venkatasamy A, Saviano A, et al. Conventional and artificial intelligence-based imaging for biomarker discovery in chronic liver disease. Hepatol Int 2022;16(3):509–22.
[39] Chan HP, Samala RK, Hadjiiski LM, et al. Deep learning in medical image analysis. Adv Exp Med Biol 2020;1213:3–21.
[40] Kuo CC, Chang CM, Liu KT, et al. Automation of the kidney function prediction and classification through ultrasound-based kidney imaging using deep learning. NPJ Digit Med 2019;2:29.
[41] Hussain MA, Hamarneh G, Garbi R. Cascaded regression neural nets for kidney localization and segmentation-free volume estimation. IEEE Trans Med Imaging 2021;40(6):1555–67.
[42] Humpire-Mamani GE, Setio AAA, van Ginneken B, et al. Efficient organ localization using multi-label convolutional neural networks in thorax-abdomen CT scans. Phys Med Biol 2018;63(8):085003.
[43] Xu X, Zhou F, Liu B, et al. Efficient multiple organ localization in CT image using 3D region proposal network. IEEE Trans Med Imaging 2019.
[44] Ishikawa M, Inoue T, Kozawa E, et al. Framework for estimating renal function using magnetic resonance imaging. J Med Imaging (Bellingham, Wash) 2022;9(2):024501.
[45] Cheng PM, Malhi HS. Transfer learning with convolutional neural networks for classification of abdominal ultrasound images. J Digit Imaging 2017;30(2):234–43.
[46] Ciompi F, de Hoop B, van Riel SJ, et al. Automatic classification of pulmonary peri-fissural nodules in computed tomography using an ensemble of 2D views and a convolutional neural network out-of-the-box. Med Image Anal 2015;26(1):195–202.
[47] Wang C, Elazab A, Wu J, et al. Lung nodule classification using deep feature fusion in chest radiography. Computerized medical imaging and graphics: the official journal of the Computerized Medical Imaging. Society 2017;57:10–8.
[48] Zheng Q, Warner S, Tasian G, et al. A dynamic graph cuts method with integrated multiple feature maps for segmenting kidneys in 2D Ultrasound images. Acad Radio 2018;25(9):1136–45.
[49] Komenda P, Rigatto C, Tangri N. Screening strategies for unrecognized CKD. Clin J Am Soc Nephrol 2016;11(6):925–7.
[50] Berns JS. Routine screening for CKD should be done in asymptomatic adults. selectively. Clin J Am Soc Nephrol 2014;9(11):1988–92.
[51] Abbasian Ardakani A, Mohammadi A, Khalili Najafabad B, et al. Assessment of kidney function after allograft transplantation by texture analysis. Iran J Kidney Dis 2017;11(2):157–64.
[52] Chen C-J, Pai T-W, Hsu H-H, et al. Prediction of chronic kidney disease stages by renal ultrasound imaging. Enterp Inf Syst 2020;14:178–95.
[53] Iqbal F., Pallewatte A.S., Wansapura J.P., editors. Texture analysis of ultrasound images of chronic kidney disease. 2017 Seventeenth International Conference on Advances in ICT for Emerging Regions (ICTer); 2017 6–9 Sept. 2017.
[54] Hao P-y, Xu Z-y, Tian S-y, et al. Texture branch network for chronic kidney disease screening based on ultrasound images. Front Inf Technol Electron Eng 2020;21(8):1161–70.
[55] Lee S, Kang M, Byeon K, et al. Machine learning-aided chronic kidney disease diagnosis based on ultrasound imaging integrated with computer-extracted measurable features. J Digit Imaging 2022.
[56] Grzywińska M, Jankowska M, Banach-Ambroziak E, et al. Computation of the texture features on T2-weighted images as a novel method to assess the function of the transplanted kidney: primary research. Transpl Proc 2020;52(7):2062–6.
[57] Kline TL, Korfiatis P, Edwards ME, et al. Image texture features predict renal function decline in patients with autosomal dominant polycystic kidney disease. Kidney Int 2017;92(5):1206–16.
[58] Dillman JR, Benoit SW, Gandhi DB, et al. Multiparametric quantitative renal MRI in children and young adults: comparison between healthy individuals and patients with chronic kidney disease. Abdom Radiol 2022;47(5):1840–52.
[59] Li XS, Zhang QJ, Zhu J, et al. Assessment of kidney function in chronic kidney disease by combining diffusion tensor imaging and total kidney volume. Int Urol Nephrol 2022;54(2):385–93.
[60] Berchtold L, Crowe LA, Combescure C, et al. Diffusion-magnetic resonance imaging predicts decline of kidney function in chronic kidney disease and in patients with a kidney allograft. Kidney Int 2022;101(4):804–13.
[61] Li LP, Leidner AS, Wilt E, et al. Radiomics-based image phenotyping of kidney apparent diffusion coefficient maps: preliminary feasibility & efficacy. J Clin Med 2022;11:7.
[62] Deng Y, Yang BR, Luo JW, et al. DTI-based radiomics signature for the detection of early diabetic kidney damage. Abdom Radiol (N Y) 2020;45(8):2526–31.
[63] Rossi C, Artunc F, Martirosian P, et al. Histogram analysis of renal arterial spin labeling perfusion data reveals differences between volunteers and patients with mild chronic kidney disease. Invest Radio 2012;47(8):490–6.
[64] Lim LS, Cheung CY, Sabanayagam C, et al. Structural changes in the retinal microvasculature and renal function. Invest Ophthalmol Vis Sci 2013;54(4):2970–6.
[65] Sabanayagam C, Shankar A, Koh D, et al. Retinal microvascular caliber and chronic kidney disease in an Asian population. Am J Epidemiol 2009;169(5):625–32.
[66] Wong CW, Wong TY, Cheng CY, et al. Kidney and eye diseases: common risk factors, etiological mechanisms, and pathways. Kidney Int 2014;85(6):1290–302.
[67] Xu X, Gao B, Ding W, et al. Retinal image measurements and their association with chronic kidney disease in Chinese patients with type 2 diabetes: the NCD study. Acta Diabetol 2021;58(3):363–70.
[68] Sabanayagam C, Xu D, Ting DSW, et al. A deep learning algorithm to detect chronic kidney disease from retinal photographs in community-based populations. Lancet Digit Health 2020;2(6):e295–302.
[69] Schley G, Jordan J, Ellmann S, et al. Multiparametric magnetic resonance imaging of experimental chronic kidney disease: a quantitative correlation study with histology. PLoS One 2018;13(7):e0200259.
[70] Haruhara K, Tsuboi N, Koike K, et al. Renal histopathological findings in relation to ambulatory blood pressure in chronic kidney disease patients. Hypertens Res 2015;38(2):116–22.
[71] Wang Y, Wen Q, Jin L, et al. Artificial intelligence-assisted renal pathology: advances and prospects. J Clin Med 2022;11(16):4918. https://doi.org/10.3390/jcm11164918
[72] Gallego J, Swiderska-Chadaj Z, Markiewicz T, et al. A U-Net based framework to quantify glomerulosclerosis in digitized PAS and H&E stained human tissues. Comput Med Imaging Graph 2021;89:101865.
[73] Weis CA, Bindzus JN, Voigt J, et al. Assessment of glomerular morphological patterns by deep learning algorithms. J Nephrol 2022;35(2):417–27.
[74] Hermsen M, de Bel T, den Boer M, et al. Deep learning-based histopathologic assessment of kidney tissue. J Am Soc Nephrol 2019;30(10):1968–79.
[75] Luciano RL, Moeckel GW. Update on the native kidney biopsy: core curriculum 2019. Am J Kidney Dis: J Natl Kidney Found 2019;73(3):404–15.
[76] Hogan JJ, Mocanu M, Berns JS. The native kidney biopsy: update and evidence for best practice. Clin J Am Soc Nephrol: CJASN 2016;11(2):354–62.
[77] Brachemi S, Bollée G. Renal biopsy practice: what is the gold standard? World J Nephrol 2014;3(4):287–94.
[78] Whittier WL, Korbet SM. Timing of complications in percutaneous renal biopsy. J Am Soc Nephrol: JASN 2004;15(1):142–7.
[79] Shi H, Jia J, Li D, et al. Blood oxygen level dependent magnetic resonance imaging for detecting pathological patterns in lupus nephritis patients: a preliminary study using a decision tree model. BMC Nephrol 2018;19(1):33.
[80] Beeman SC, Cullen-McEwen LA, Puelles VG, et al. MRI-based glomerular morphology and pathology in whole human kidneys. Am J Physiol Ren Physiol 2014;306(11):F1381–90.
[81] Zhu M, Ma L, Yang W, et al. Elastography ultrasound with machine learning improves the diagnostic performance of traditional ultrasound in predicting kidney fibrosis. J Formos Med Assoc = Taiwan yi zhi 2022;121(6):1062–72.
[82] Srivastava A, Palsson R, Kaze AD, et al. The prognostic value of histopathologic lesions in native kidney biopsy specimens: results from the boston kidney biopsy Cohort study. J Am Soc Nephrol: JASN 2018;29(8):2213–24.
[83] Mariani LH, Martini S, Barisoni L, et al. Interstitial fibrosis scored on whole-slide digital imaging of kidney biopsies is a predictor of outcome in proteinuric glomerulopathies. Nephrol, Dial, Transpl: Publ Eur Dial Transpl Assoc - Eur Ren Assoc 2018;33(2):310–8.
[84] Albaradei S, Thafar M, Alsaedi A, et al. Machine learning and deep learning methods that use omics data for metastasis prediction. Comput Struct Biotechnol J 2021;19:5008–18.
[85] Daginawala N, Li B, Buch K, et al. Using texture analyses of contrast enhanced CT to assess hepatic fibrosis. Eur J Radiol 2016;85(3):511–7.
[86] Yu H, Buch K, Li B, et al. Utility of texture analysis for quantifying hepatic fibrosis on proton density MRI. J Magn Reson Imaging: JMRI 2015;42(5):1259–65.
[87] Zhang X, Gao X, Liu BJ, et al. Effective staging of fibrosis by the selected texture features of liver: Which one is better, CT or MR imaging? Comput Med Imaging Graph: J Comput Med Imaging Soc 2015;46(Pt 2):227–36.
[88] Yu Y, Wang J, Ng CW, et al. Deep learning enables automated scoring of liver fibrosis stages. Sci Rep 2018;8(1):16016.
[89] Anteby R, Klang E, Horesh N, et al. Deep learning for noninvasive liver fibrosis classification: a systematic review. Liver Int 2021;41(10):2269–78.
[90] Yasaka K, Akai H, Kunimatsu A, et al. Deep learning for staging liver fibrosis on CT: a pilot study. Eur Radio 2018;28(11):4578–85.
[91] Wang K, Lu X, Zhou H, et al. Deep learning Radiomics of shear wave elastography significantly improved diagnostic performance for assessing liver fibrosis in chronic hepatitis B: a prospective multicentre study. Gut 2019;68(4):729–41.
[92] Hectors SJ, Kennedy P, Huang KH, et al. Fully automated prediction of liver fibrosis using deep learning analysis of gadoxetic acid-enhanced MRI. Eur Radio 2021;31(6):3805–14.
[93] Yin Y, Yakar D, Dierckx R, et al. Liver fibrosis staging by deep learning: a visual-based explanation of diagnostic decisions of the model. Eur Radio 2021;31(12):9620–7.
[94] Chantaduly C, Troutt HR, Perez Reyes KA, et al. Artificial intelligence assessment of renal scarring (AIRS Study). Kidney360 2022;3(1):83–90.

[95] Widjaja E, Oxtoby JW, Hale TL, et al. Ultrasound measured renal length versus low dose CT volume in predicting single kidney glomerular filtration rate. Br J Radiol 2004;77(921):759–64.
[96] Jagtap JM, Gregory AV, Homes HL, et al. Automated measurement of total kidney volume from 3D ultrasound images of patients affected by polycystic kidney disease and comparison to MR measurements. Abdom Radio 2022;47(7):2408–19.
[97] Daniel AJ, Buchanan CE, Allcock T, et al. Automated renal segmentation in healthy and chronic kidney disease subjects using a convolutional neural network. Magn Reson Med 2021;86(2):1125–36.
[98] van Gastel MDA, Edwards ME, Torres VE, et al. Automatic measurement of kidney and liver volumes from MR images of patients affected by autosomal dominant polycystic kidney disease. J Am Soc Nephrol 2019;30(8):1514–22.
[99] Kim Y, Tao C, Kim H, et al. A deep learning approach for automated segmentation of kidneys and exophytic cysts in individuals with autosomal dominant polycystic kidney disease. J Am Soc Nephrol 2022;33(8):1581–9.
[100] Conze PH, Kavur AE, Cornec-Le Gall E, et al. Abdominal multi-organ segmentation with cascaded convolutional and adversarial deep networks. Artif Intell Med 2021;117:102109.
[101] Yin S., Zhang Z., Li H., et al. FULLY-AUTOMATIC SEGMENTATION OF KIDNEYS IN CLINICAL ULTRASOUND IMAGES USING A BOUNDARY DISTANCE REGRESSION NETWORK. Proceedings IEEE International Symposium on Biomedical Imaging. 2019;2019:1741–4.
[102] Sharma K, Rupprecht C, Caroli A, et al. Automatic segmentation of kidneys using deep learning for total kidney volume quantification in autosomal dominant polycystic kidney disease. Sci Rep 2017;7(1):2049.
[103] Onthoni DD, Sheng TW, Sahoo PK, et al. Deep learning assisted localization of polycystic kidney on contrast-enhanced CT images. Diagn (Basel) 2020;10(12):1113.
[104] Kim Y, Tao C, Kim H, et al. A deep learning approach for automated segmentation of kidneys and exophytic cysts in individuals with autosomal dominant polycystic kidney disease. J Am Soc Nephrol 2022;33(8):1581–9.
[105] Raj A, Tollens F, Hansen L, et al. Deep learning-based total kidney volume segmentation in autosomal dominant polycystic kidney disease using attention, cosine loss, and sharpness aware minimization. Diagn 2022;12(5):1159.
[106] Kline TL, Edwards ME, Fetzer J, et al. Automatic semantic segmentation of kidney cysts in MR images of patients affected by autosomal-dominant polycystic kidney disease. Abdom Radio 2021;46(3):1053–61.
[107] Sharbatdaran A, Romano D, Teichman K, et al. Deep learning automation of kidney, liver, and spleen segmentation for organ volume measurements in autosomal dominant polycystic kidney disease. Tomography 2022;8(4):1804–19.